Journal of Engineering Issues and Solutions

Probabilistic seismic hazard analysis of Nepal considering validated seismic source model

Agriya Sagar Pandit[1], Dilendra Prasad Joshi[1,*], Chetana Subedi[1], Alisha Poudel[1], Roshan Sharma[1], Pawan Chhetri[1]

[1] *Department of Civil Engineering, Paschimanchal Campus, Institute of Engineering, Tribhuvan University*

**Corresponding email: joshidilendilu@gmail.com*

Received: April 30, 2024; Revised: June 09, 2024; Accepted: June 15, 2024

doi: https://doi.org/10.3126/joeis.v3i1.65322

Abstract

Earlier studies have performed Probabilistic Seismic Hazard Analysis (PSHA) of Nepal considering different source models. This study aims to validate the best seismic source model to perform PSHA in Nepal. Earthquake data from earthquake catalogues for the period of 1900 to 2022 AD has been considered. The earthquake data obtained from catalogues was homogenised and merged. De-clustering was performed to remove dependent events using ZMAP. A completeness test was performed and recurrence parameters were computed. As proposed in earlier studies, Peak Ground Acceleration (PGA) values were calculated for 3D source, fault source and areal sources for 6.36% probability of exceedance for 50 years. A comparison was made between the PGA values of all source models with the recorded PGA value of the Kirtipur (KTP) station for the 2015 Gorkha Earthquake for a 760-year return period. The comparison of PGA values proves the Single Ramp Model (SRM) of the Main Himalayan Thrust (MHT) to be the validated seismic source model for Nepal. PSHA was then performed with the validated source model and hazard maps were prepared for 2% and 10% probability of exceedance. The analysis revealed that PGA values reached maximum levels in the far western and central regions. Using a single ramp model of MHT with improved Ground Motion Prediction Equations (GMPEs) specific to the Himalayan region is necessary for future seismic hazard analysis.

Keywords: *MHT, PGA, PSHA, source models.*

1. Introduction

Nepal is located on the border between the Indian and Eurasian tectonic plates, in an area that experiences frequent earthquake activity (Upreti, 1999). According to Ader et al. (2012), the movement of the Indian plate as it converges with and subducts beneath the Eurasian plate is about 5 cm per year. The collision between these two plates has led to the formation of the Himalayan Mountain range and the convergence has resulted in the occurrence of seismic events along the Himalayan belt. The geological features in Nepal,

such as faults and thrusts, play a significant role in earthquakes. Main Himalayan Thrust (MHT) plays a significant role in earthquake nucleation and propagation (Hubbard et al., 2016). These faults accommodate the deformation of the Earth's crust and are associated with the tectonic forces at play.

Nepal, being centrally located in the Himalayas, experiences a significant number of earthquakes each year, with magnitudes exceeding 4 moment magnitude (M_W). While most of these earthquakes fall within the magnitude (M_W) range of 4 to 6, they usually do not result in significant damage. It is worth noting that earthquakes of magnitude M_W 6.5 or higher are the ones known to cause damage in Nepal (Prakash, 2016). The plate tectonics is dominated by three master thrusts, the Main Frontal Thrust, the Main Boundary Thrust, and the Main Central Thrust. All of these thrusts come together at the same depth in a low-angle decollement known as The Main Himalayan Thrust (Upreti, 1999). Figure 1 depicts the locations of faults and places of occurrence of major historical earthquakes in Nepal.

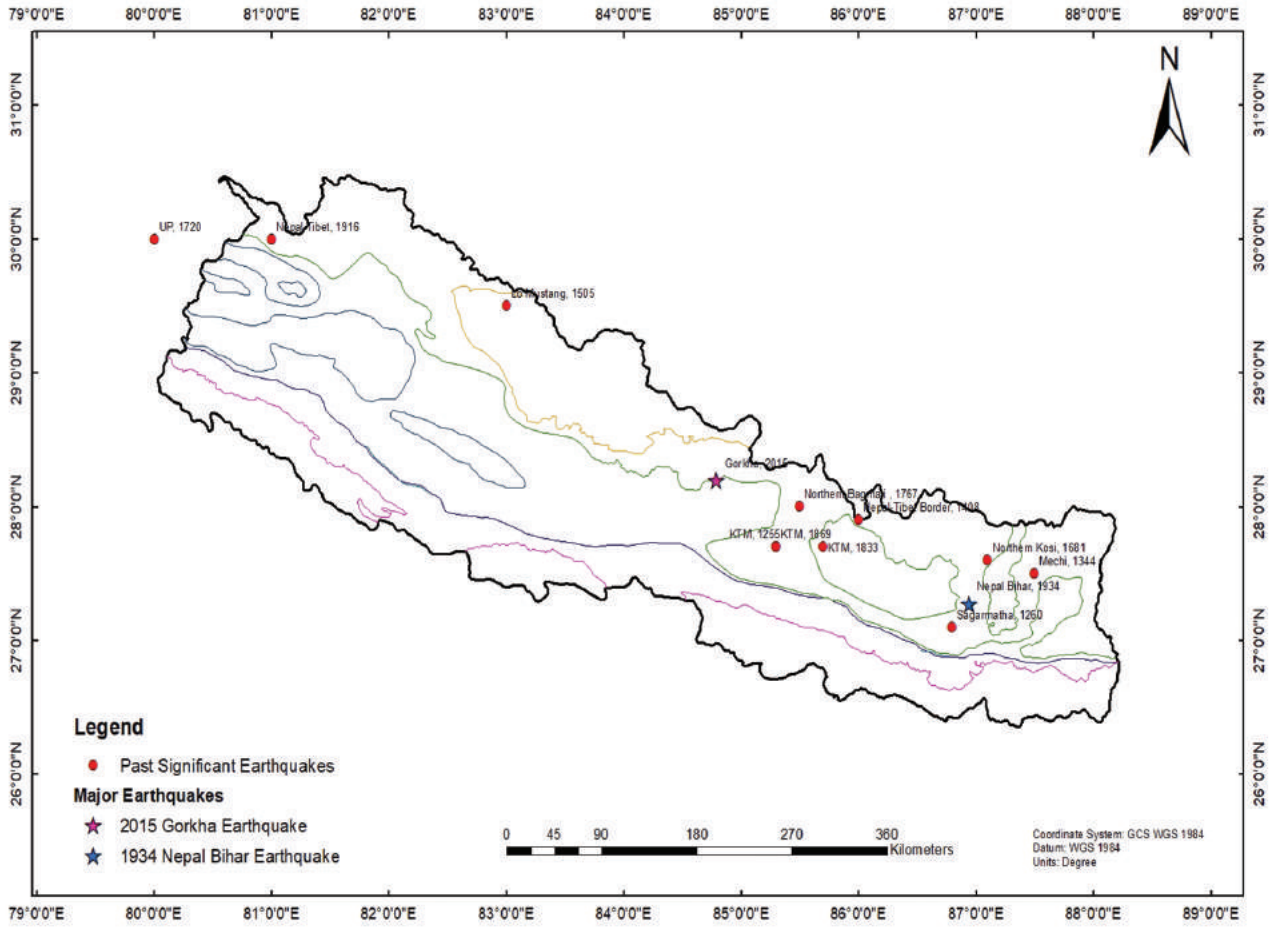

Figure 1: Map of Nepal depicting faults and major historical earthquakes

To understand earthquake patterns and ensure public safety, the design of earthquake-resistant buildings and resilient infrastructures is crucial. Probabilistic Seismic Hazard Analysis (PSHA) has been performed considering different seismic source models for Nepal (2D, 3D, linear source model) (e.g. Parajuli, 2015; Hubbard et al., 2016; Rahman & Bai, 2018; Stevens et al., 2018; Niraula & Chamlagain, 2020; Chamlagain et.al., 2020).

PSHA assesses the likelihood and intensity of an earthquake in a particular region based on factors such as historical earthquake data, seismological information, geological data and mathematical modelling (Baker et al., 2021). There is a need for improved hazard assessment through accurate estimation of seismic hazard considering proper geometry of earthquake source. This study aims to validate the best seismic source model specific to Nepal and use it to develop a probabilistic seismic hazard map and hazard curve for seismic code applications specific to Nepal.

2. Materials and Methods

The study area encompasses the entire region of Nepal taking into account its tectonic setting, fault systems, seismicity rates, geology, and site effects. PSHA is a probabilistic framework used in the calculation of the probabilities of ground shaking occurring at various levels within a specific period. The analysis involves determining the rates of earthquake occurrence, magnitudes of potential earthquakes, and the attenuation of ground shaking with distance from the seismic source. The process of PSHA typically involves the characterization of seismic sources, ground motion prediction, hazard calculation, uncertainty analysis, and hazard mapping. Cornell (1968) and Algermissen et al. (1982) made significant contributions by developing the initial mathematical framework for PSHA. PSHA is a useful instrument for evaluating seismic risks and is frequently applied to infrastructure and engineering projects. The steps involved in the PSHA process are shown in Figure 2**.**

2.1 Data collection

Earthquake catalogue data is compiled from reputable sources like the International Seismological Center (ISC), Global Centroid Moment Tensor (GCMT), United States Geological Survey (USGS), and Department of Mines and Geology (DMG) covering earthquakes from 1900 to 2022 in the region between longitudes 79° E and 90° E and latitudes 26° N and 31.7° N. The catalogue includes earthquakes above magnitude 4 up to a depth of 322 km, with improved data quality since 1964. It consists of various magnitude types and comprises both main events and aftershocks. Since 1964, the database's quality has greatly increased. Smaller-magnitude earthquake data was incomplete and inaccurate before 1964. Different forms of magnitude (local magnitude, body wave, surface, duration, and moment) and a combination of main events and aftershocks make up the assembled seismicity library.

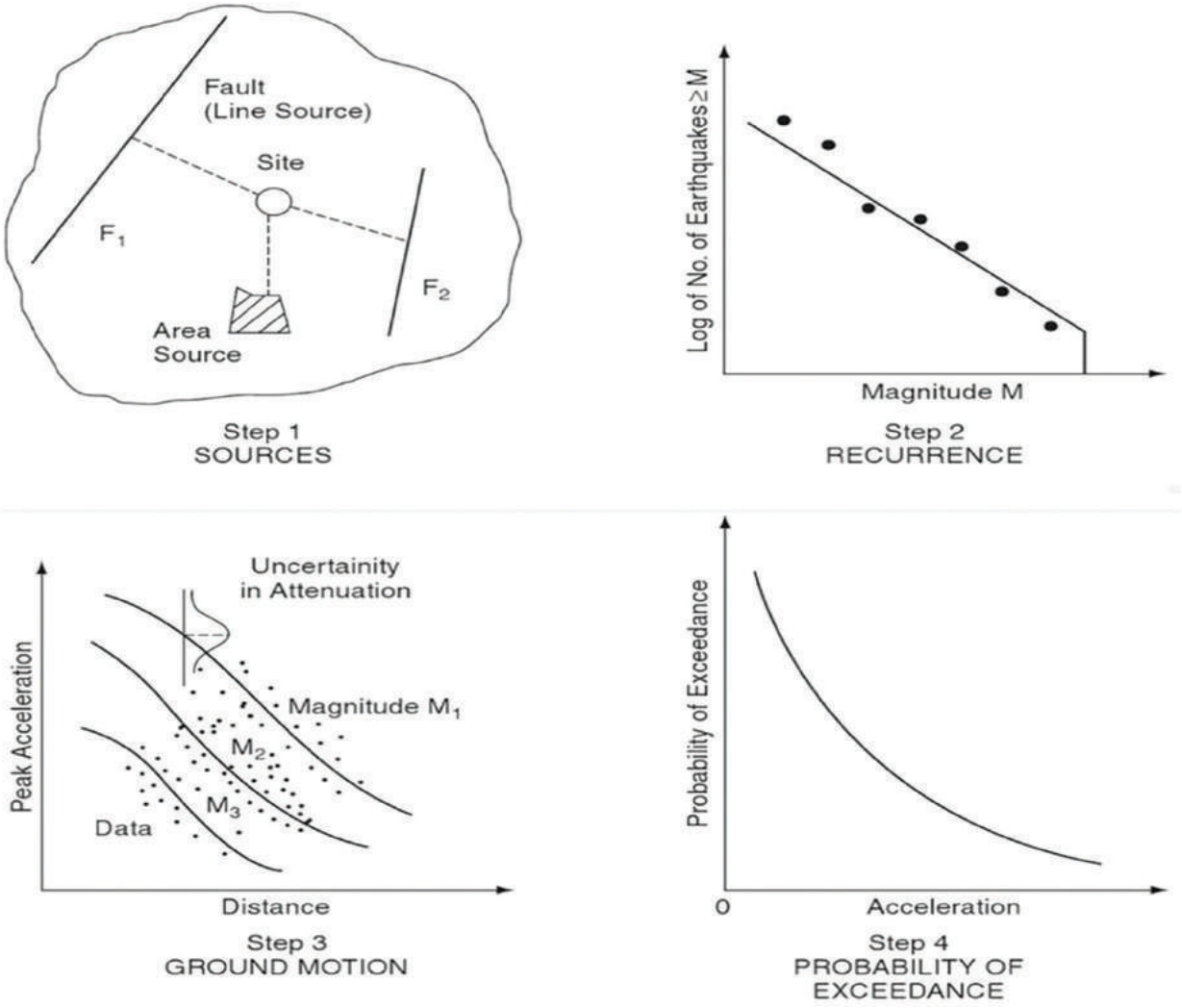

Figure 2: Four steps of a probabilistic seismic hazard analysis (Reiter 1990)

DMG earthquake catalogue spans from 1994 to 2018, with 2557 earthquakes of magnitude M_W 4.0 or higher, predominantly in the 4.0 - 5.0 range. GCMT's catalogue from 1979 to 2022 includes 128 earthquakes of magnitude M_W 4.0 or higher, primarily in the 5.0 - 6.0 range. ISC's catalogue from 1916 to 2022 features 2627 earthquakes, with a similar distribution to DMG's. USGS's catalogue from 1911 to 2022 contains 1365 earthquakes, with a majority falling in the range of M_W 4.0 - 5.0. A total of 6677 earthquake data was collected from earthquake catalogues as shown in Figure 3.

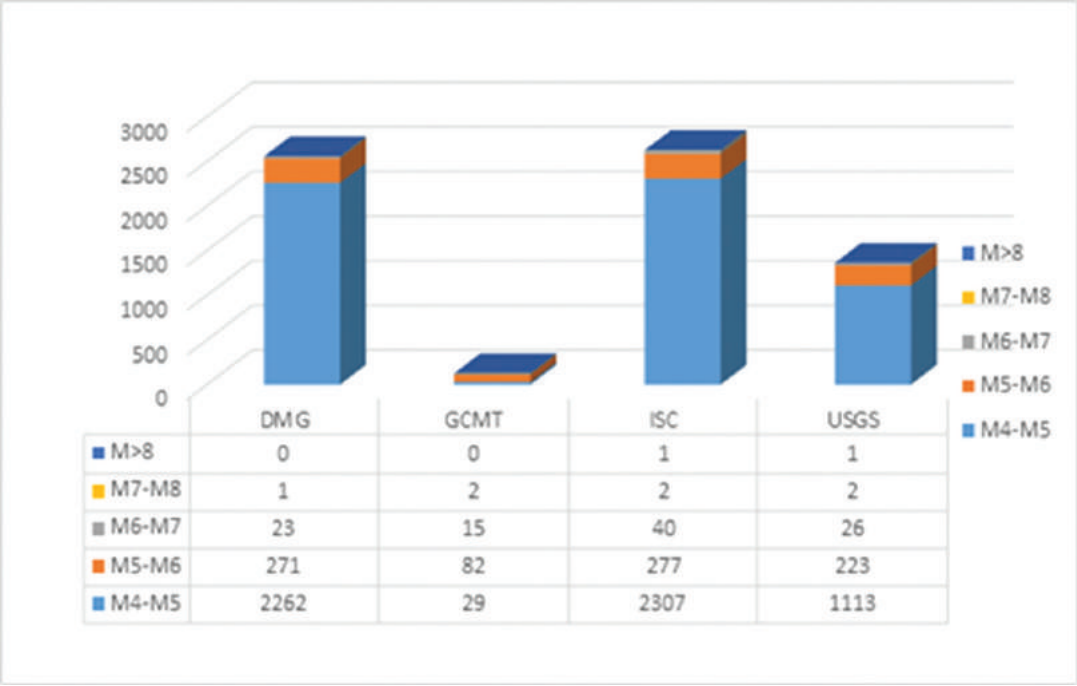

	DMG	GCMT	ISC	USGS
M>8	0	0	1	1
M7-M8	1	2	2	2
M6-M7	23	15	40	26
M5-M6	271	82	277	223
M4-M5	2262	29	2307	1113

Figure 3. Earthquake catalogues from DMG, GCMT, ISC and USGS

2.2 Homogenization and merging

Historic earthquake catalogues collected from different sources (ISC, USGS, GCMT and DMG) have different magnitude types (surface magnitude (M_S), local magnitude (M_L), body magnitude (M_B), and duration magnitude (M_D)). These magnitudes are converted to a common Moment Magnitude (M_W) using convergence equations given by Nath et al. (2016) and Ader et al. (2012). Python code is written to convert the catalogues to common moment magnitude.

Following Thingbaijam et al. (2009), probable duplication of occurrences is removed by looking for events that happen within a 90-kilometer radius on the same day, hour, and minute and keeping the event with the biggest magnitude. The priority for homogenization was in the increasing order of ISC, USGS, GCMT and DMG. Following homogenization and merging, the number of data is reduced from 6677 to 4211. Figure 4 represents earthquake data in a map of Nepal prepared in ArcGIS after merging.

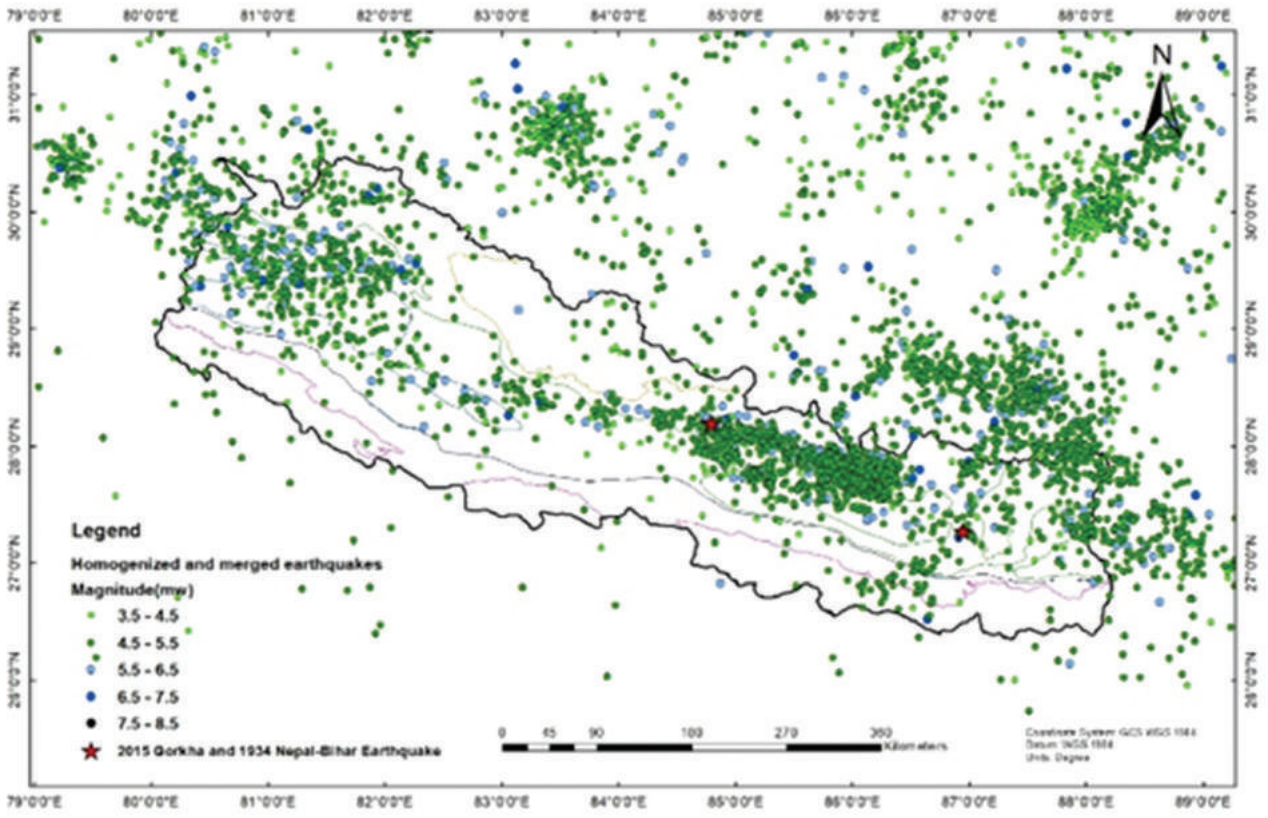

Figure 4: Earthquake data after merging

2.3 Declustering of catalogue

Declustering is the process of deleting aftershocks and other dependent events from combined earthquake databases. Since these occurrences are too weak to affect seismicity through a strong ground motion, they are eliminated according to Gardner & Knopoff's technique (1974).

The earthquake record often includes a significant number of aftershocks, which, if not excluded, can cause the earthquake data to deviate from a Poisson distribution. This non-Poissonian behaviour complicates the statistical analysis. Therefore, a method called the windowing algorithm, introduced by Gardner and Knopoff in 1974, is employed in ZMAP for the identification and removal of aftershocks. Algorithm is identified by the aftershocks by considering their distance from the epicentre of the main shock and the time difference between their occurrences and the main shock. After applying the windowing algorithm to remove the aftershocks, the resulting earthquake catalogue confirms more closely to a Poisson distribution.

The raw data contained 4211 events and out of them, 1756 were independent events. The de-clustered catalogues are used for further seismic hazard analysis. Figure 5 represents earthquake data in a map of Nepal prepared in ArcGIS after declustering.

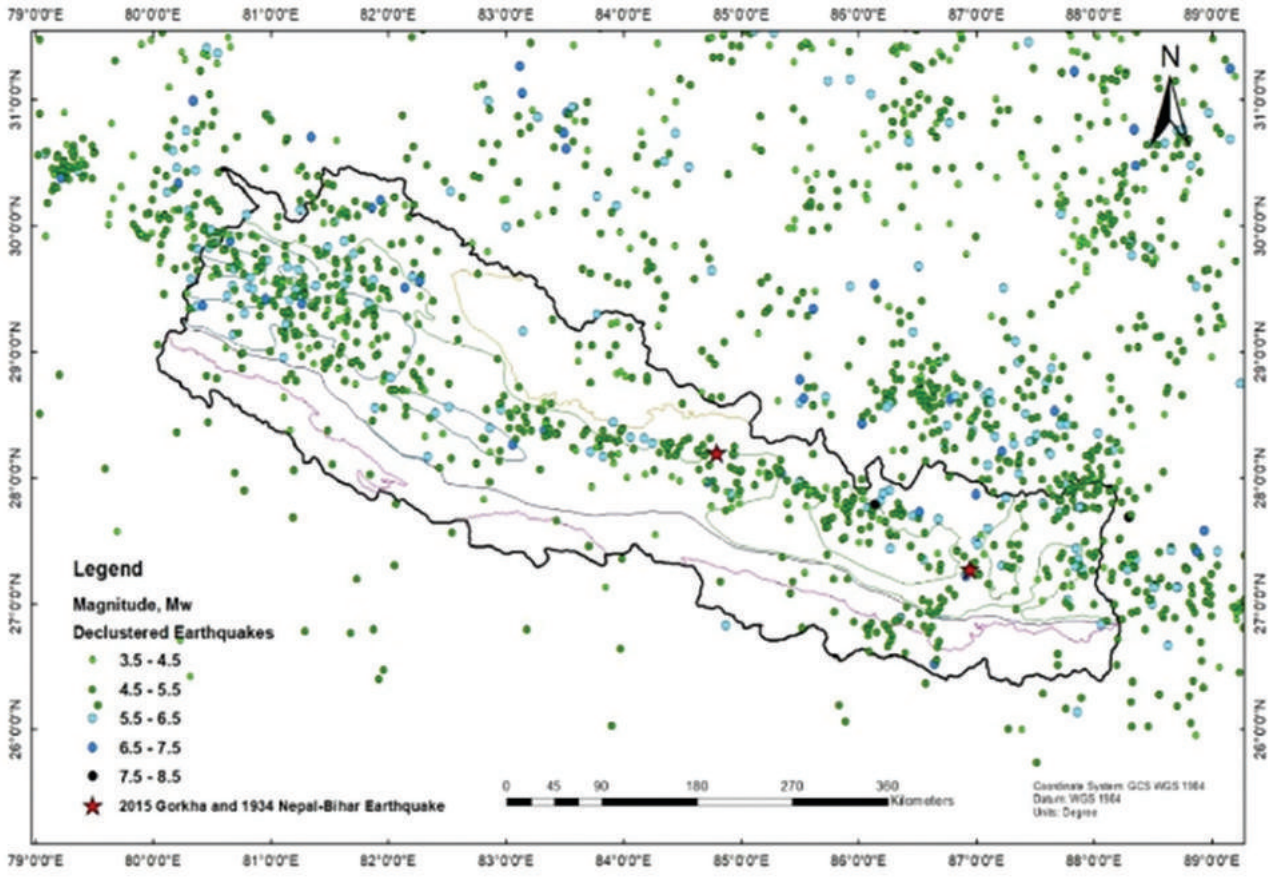

Figure 5: Earthquake data after declustering

2.4 Source characterization

Determining the frequency of earthquakes at a given site with a certain magnitude and dimension is known as source characterization. Calculating the recurrence rate for each scenario involves developing a series of probable earthquake scenarios, complete with magnitude, dimension, and location. Modelling the seismic sources' geometry is the first stage in source characterization. Two commonly used approaches are the areal source zone method and the fault source method. The areal source zone method defines source regions based on geographic boundaries, while the fault source method focuses on modelling specific fault structures (Baker et al., 2021). After establishing the geometry, models are developed which assist in the description of various aspects of earthquake occurrence. These models incorporate various aspects such as the distribution of magnitudes of earthquakes, the rupture dimensions distribution associated with each magnitude, the spatial distribution of earthquake locations of each rupture dimension, and the rate of occurrence of earthquakes on the source, considering a minimum magnitude threshold of interest. These models provide insights into the likelihood and characteristics of earthquakes in a particular area.

For this study, sources are broadly categorized into three source models. 3D source model given by Niraula and Chamlagain (2020), linear source model (i.e., fault source) given by Rahman and Bai (2018) and Stevens et al. (2018), and areal sources model given by Ghimire and Parajuli (2016), Chaulagain et al. (2015), Niraula and Chamlagain (2020) and Stevens et al. (2018) have been considered for the study after an intensive literature

review. Spatially distributed maps of all these sources are provided in Annex 1 - Source Characterization.

2.5 Completeness test

To obtain realistic earthquake recurrence parameters, a completeness test is conducted using the earthquake catalogue for each seismic source. It is performed to determine the magnitude threshold below which earthquakes are unlikely to be reliably detected and recorded in the catalogue. Determining the precise location of earthquake occurrences and assigning them to specific faults can be challenging. Additionally, the availability of earthquake data from older times is often limited, leading to uneven distribution in the number of recorded earthquakes. To address these challenges and ensure accurate analysis, it is crucial to conduct a completeness analysis to determine the best-fit frequency formula. This approach is based on the study by Stepp in 1972.

2.6 G-R parameters

The 'G-R relationship' typically refers to the Gutenberg-Richter relationship, which is a fundamental empirical law in seismology that describes the statistical distribution of earthquake magnitudes in a given region. It is named after the seismologists Beno Gutenberg and Charles F. Richter, who independently developed the relationship.

The Gutenberg-Richter relationship states that, in a specific region, the logarithm of the number of earthquakes of a given magnitude (M) is proportional to the magnitude itself. Mathematically, it can be expressed as:

$$\log(N) = a - bM \quad (1)$$

Where: log(N) is the logarithm of the number of earthquakes with magnitude greater than or equal to M; a is a constant representing the number of earthquakes at a reference magnitude (usually 0); b is a constant called the Gutenberg-Richter (GR) b-value, which characterizes the rate of decrease in the number of earthquakes with increasing magnitude.

The Gutenberg-Richter relationship indicates that there are many small earthquakes and fewer large earthquakes. The b-value provides information about the relative frequency of small versus large earthquakes in a particular region. A lower b-value indicates a relatively higher proportion of larger earthquakes, while a higher b-value indicates a greater proportion of smaller earthquakes.

The completeness magnitude M_C is theoretically defined as the lowest magnitude at which 100% of the earthquakes in a space-time volume are detected (Rydelek and Sacks 1989). Correct estimation of M_C is essential for any seismicity analysis, as it has an impact on the b-value parameter. The Maximum Likelihood Method (MLM) (Aki, 1965), Least Square Method (LSM) and Maximum Curvature Method (MCM) using the ZMAP package (Wiemer and Wyss 2000) are used to estimate the b-value. MCM sometimes underestimates the seismicity parameters, and since the globally accepted b-value is nearer to 1 (Mignan & Woessner (2012), Khanal et al. (2023)), by comparing the values from all the methods, the final b-value is chosen for further analysis.

2.7 Ground motion prediction equations (GMPEs) and logic tree

So far, a ground motion prediction equation has not been developed specifically for the seismic scenario in Nepal. GMPEs are developed based on empirical observations and statistical analysis of recorded ground

motions from past earthquakes. These equations consider various factors that influence ground motion, including earthquake magnitude, distance from the earthquake source, site conditions, and path effects. They provide a relationship between these input parameters and the expected ground motion levels.

PSHA comprises several epistemic uncertainties which affect the process of hazard analysis (Bhusal & Parajuli, 2019). There is a lack of clear definition of earthquake sources and GMPEs. So, a combination of different GMPEs and sources is used to minimize error. Logic trees can efficiently handle epistemic uncertainties present in source model and attenuation relation (Power et al. 1981, Kulkarni et al. 1984, and Coppersmith & Youngs, 1986). A logic tree is an effective way to incorporate multiple models in terms of sources, GMPEs, and seismicity parameters by assigning suitable probability factors for each alternative based on their occurrence. The relative credibility of each alternative model is represented by the probabilities. The probabilities give a sum of unity at each branch (Bhusal and Parajuli, 2019). Logical trees have applicability not only for GMPEs and sources but also for multiple seismic parameters, maximum magnitude, magnitude distribution, and recurrence law. In this study, two categories of seismological sources (2D source and 3D source) and three sets of GMPEs, Subduction Interference, Active Shallow Crust and Stable Continental Area with eight GMPEs, are combined by the use of a logical tree along with weightage assigned based on their nature and personal judgement.

2.8 Validation

Values of PGA for a 6.36% probability of exceedance for 50 years were calculated for 3D sources, fault sources, and areal sources as proposed by various authors using the OpenQuake Engine. The values obtained were compared to the recorded strong ground motion at KTP station during the 2015 Gorkha Earthquake. The comparison of PGA values obtained from different source models for 50 years with a 6.36% probability of exceedance considered is shown in Table 1.

Table 1: Computed PGA of different sources along with % error with respect to KTP

S. N.	Source Model	Calculated PGA	% Error with respect to KTP
1	MHT considering geometry (SRM 3D Source) (Chamlagain, 2020)	0.253 g	2.7%
2	Stevens et al. (2018) (Fault)	0.250 g	3.8%
3	Rahman and Bai (2018) (Fault)	1.5 g	476%
4	Chaulagain et al. (2015) (Areal)	0.269 g	3.5%
5	Stevens et al. (Areal)	0.314 g	20.8%
6	Ghimire and Parajuli (2016) (Areal)	0.251 g	3.5%

From Table 1, we can see that the value of PGA obtained from the Single Ramp Model (3D Source Model), i.e. 0.253 g is closest to that of PGA recorded at KTP station during the 2015 Gorkha earthquake i.e. roughly 0.26 g (Takai et al., 2016). The model used by Stevens et al. (2018) does not consider the declustering of catalogues which tends to deviate from the values of parameters obtained. Chaulagain et al. (2015) do not consider the subduction sources for performing PSHA. Rahman and Bai have taken a shorter length of catalogues which might be the reason for the variation in the value of PGA.

Thus, the best source model turns out to be the Single Ramp Model of MHT (3D Source model). This is

because the model has given proper consideration to the Subduction sources. It has also considered the locked portion of the MHT fault as a separate fault source which tends to give better results (Chamlagain et al., 2020).

3. Results and Discussion

The OpenQuake codes developed by the Global Earthquake Model (GEM) are used in this project for hazard estimation. OpenQuake is a software that performs seismic hazard assessment based on the logic tree approach. The inputs required are source models, geometry, magnitude-frequency statistics, site locations, site parameters, and essential GMPEs. The source model created here can incorporate point source, area source, simple fault source, grid source, and fault ruptures that incorporate complex fault geometry realistically.

The GMPEs and source models are combined through a logic tree and the weightage is modelled in the GEM OpenQuake engine. The average value of shear wave velocity measured at a depth of 30 m (Vs_{30}) at the bedrock level is used to incorporate site effects in hazard level, as per the demand of each GMPE considered. The site-specific computation of seismic hazard (Cornell, 1968) is carried out for both single and double ramp geometries, fault geometries, and areal sources in OpenQuake for 760 years return period, which is the approximate return period for large magnitude earthquakes in Nepal (Niraula & Chamlagain, 2020).

3.1 3-D source model

The single ramp model or the double ramp model for MHT does not show any considerable variation in PSHA (Chamlagain et al. 2020). In our study, we have considered the Single Ramp Model for subduction interface (MHT) and PGA at the KTP station for 760 years return period is computed. The PGA at the KTP station is found to be 0.253 g which is approximately equal to the PGA value computed by Chamlagain et al. (2020) and close to the PGA value recorded at the KTP station (0.26 g). Further, the PGA is also computed without considering the geometry of MHT which shows no significant difference in PGA value.

3.2 Areal source model

Stevens et al. (2020) used four active shallow crust GMPEs viz., Chiou and Youngs (2014) and Boore et al. (2014), Chiou and Youngs (2008) and Boore and Atkinson (2008) with equal weightage for areal sources. Since the study does not incorporate the declustering process, there is variation in a- and b- parameters. Further, the calculated PGA for the KTP station is 0.314 g for a 6.36% probability of exceedance for 50 years which is higher as compared to PGA observed during the 2015 Gorkha earthquake, i.e. roughly 0.26 g (Takai et al., 2016), indicating an insignificant contribution of areal source for hazard computation.

Ghimire and Parajuli (2016) used three GMPEs developed for the Subduction Interface Zone viz., Young's et al. 1997, Kanno et al. 2006, and Zhao et al. 2006 with equal weightage. Due to variation in uncertainties, there is variation in a- and b- parameters. Further, the calculated PGA for the KTP station is 0.251 g for a 6.36% probability of exceedance for 50 years which is lower as compared to the PGA observed during the 2015 Gorkha earthquake i.e. roughly 0.26 g (Takai et al., 2016) indicating ignorable contribution of areal source for hazard computation.

Chaulagain et al., (2015) used five GMPEs developed for the Active Shallow Crust and Subduction Interface Zone viz., Boore and Atkinson (2003), Youngs et. al. (1997), Campbell and Bozorgnia (2008), Chiou and Youngs (2008), and Boore and Atkinson (2008) with equal weightage. Due to a lack of consideration of the subduction sources, there is variation in a- and b- parameters. Further, the calculated PGA for the KTP station is 0.269 g for a 6.36% probability of exceedance for 50 years which is higher as compared to the PGA

observed during the 2015 Gorkha earthquake i.e. roughly 0.26 g (Takai et al., 2016) indicating the lower contribution of areal source for hazard computation.

3.3 Fault source model

Stevens et al. (2018) used four subduction interface GMPEs viz., Abrahamson et al. (2016), Atkinson & Boore (2003), Boore et al. (2014), and Zhao et al. (2006) with equal weightage for fault sources. Since the study does not incorporate the declustering process there is variation in a- and b- parameters. Further, PGA for the KTP station has been calculated to be 0.251 g for a 6.36% probability of exceedance in 50 years which is lower as compared to PGA observed during the 2015 Gorkha earthquake i.e. roughly 0.26 g (Takai et al., 2016). Since we have declustered the earthquake catalogues which might be the reason for the variation in PGA.

Rahman and Bai (2018) used four subduction interface GMPEs viz., Abrahamson et al. (2016), Atkinson & Boore (2003), Youngs et al. (1997) and Zhao et al. (2006) with equal weightage for fault sources. Short catalogues (55-56) give low hazard values in certain regions where great earthquakes occur (Bilham, 2015). The PGA for the KTP station has been calculated as 1.5 g for a 6.36% probability of exceedance for 50 years which is high as compared to the PGA observed during the 2015 Gorkha earthquake i.e. roughly 0.26 g (Takai et al., 2016). The reason for this deviation is that we have considered long catalogues of 123 years which overestimates the hazard value.

3.4 Hazard map

The hazard estimate for a 10% probability of exceedance for 50 years shows a large variation in the values of PGA and the maximum hazard value is as high as 0.5 g. Areas of the far western, central, and eastern parts of Nepal fall into high hazard zone which is shown in Figure 6 and Figure 7. This region has a high rate of seismicity compared to various other regions of Nepal. In central Nepal and near the Kathmandu valley, peak hazard values range up to 0.4 g. For far-western Nepal, hazard values were as high as 0.5 g. Numerous studies (Avouac et al., 2015; Rajendran et al., 2015; Sapkota et al., 2013) have pointed to MHT as the source potentially producing earthquakes of great intensities in Nepal.

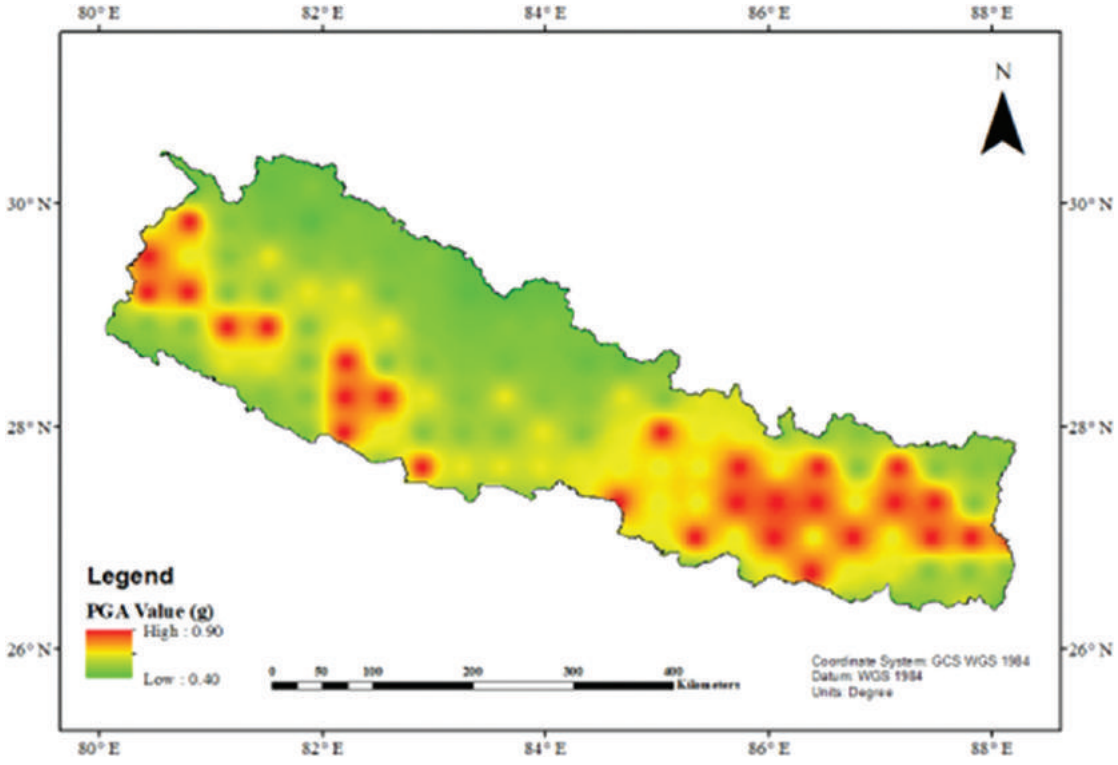

Figure 6: PSHA map for 2% probability of exceedance in 50 years

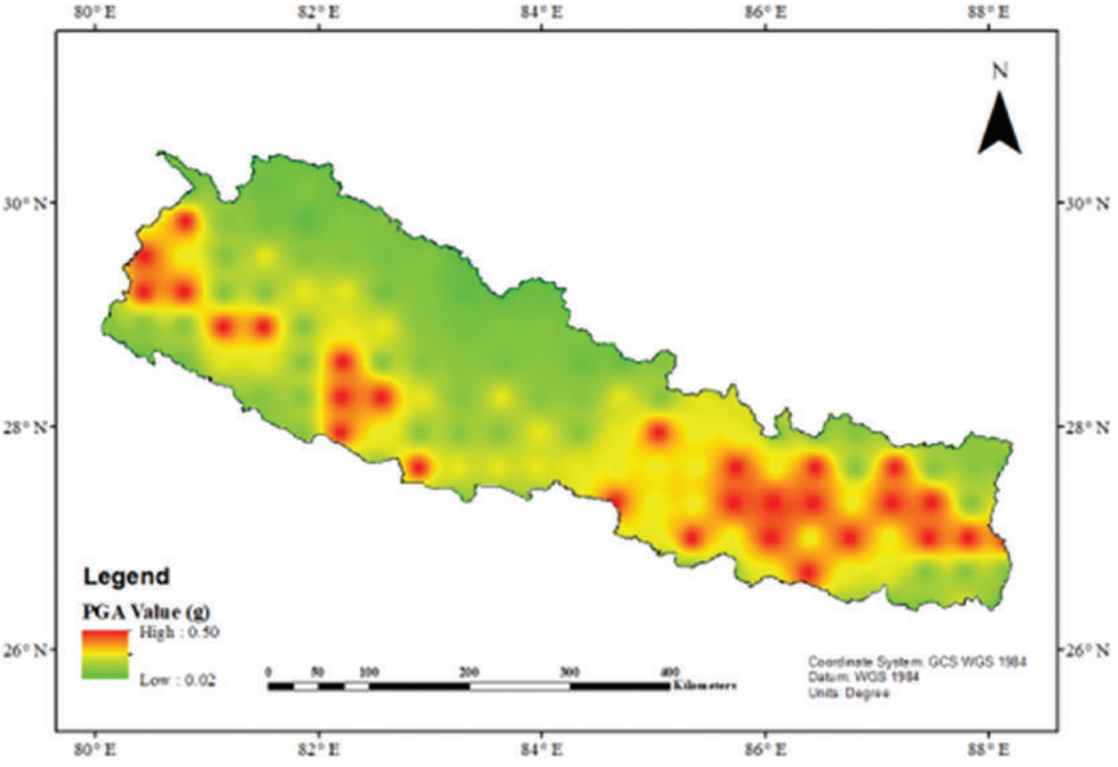

Figure 7: PSHA map for 10% probability of exceedance in 50 years

3.5 Hazard curve

In PSHA, hazard curves play a pivotal role in quantifying the seismic risk for a specific location. Hazard curves are used for the determination of the annual probability of occurrence of each of these ground motions. Hazard curves for various return periods are extracted from the OpenQuake.

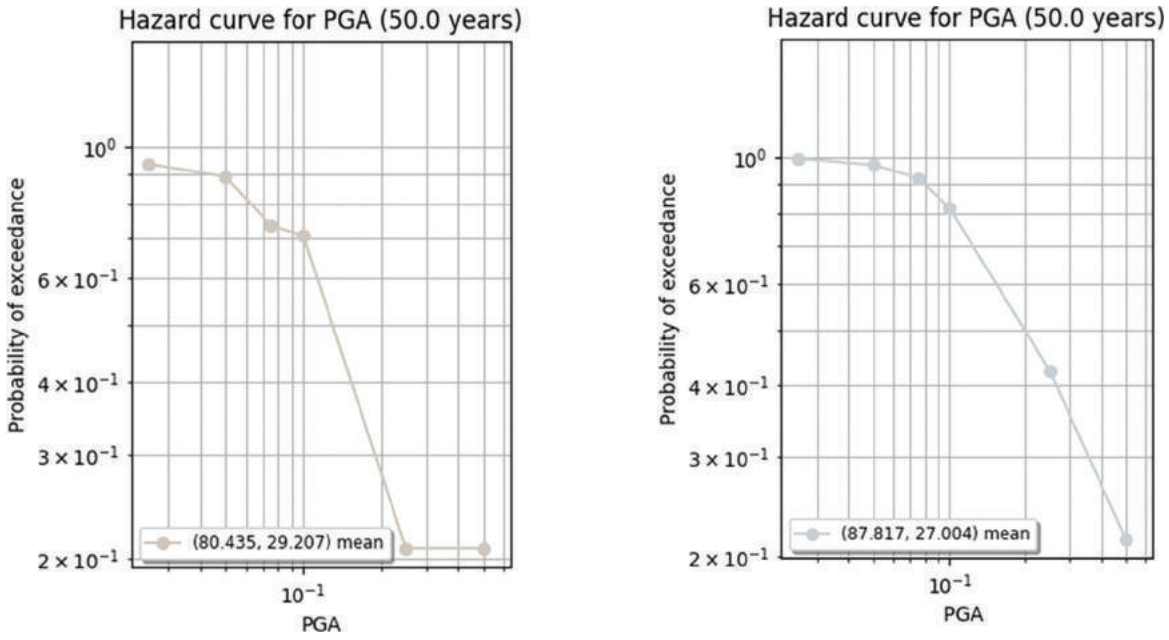

Figure 8: Hazard curve for 10 % probability of exceedance in 50 years for Dadeldhura (Far-western region) and Illam (Eastern region)

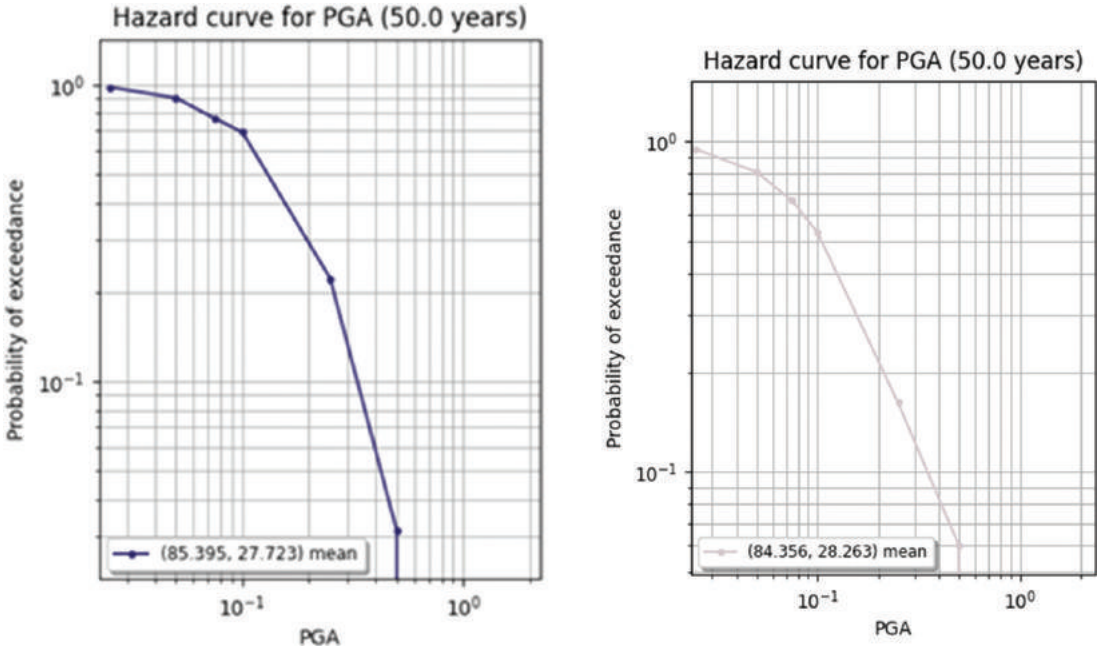

Figure 9: Hazard curve for 10 % probability of exceedance in 50 year for Kaski and Kathmandu

The graph shows that the value of PGA and probability of exceedance is inversely proportional to each other. As the value of PGA increases, the probability of exceedance decreases and vice versa. Mostly, a 10% probability of exceedance is used for major structures and a 2% probability of exceedance is used for minor structures (NBC 105).

3.6. Comparison of computed PGA with PGA mentioned in NBC-105

Table 2 presents a comparison of computed and tabulated NBC values of PGA for major cities of Nepal. A comparison of PGA values of NBC-105, 2020 with PGA values computed in this study reflect that the values computed are close to the values mentioned in the code.

Table 2: Comparison of computed PGA with PGA mentioned in NBC-105

S. No.	City	PGA computed	PGA from NBC
1	Kathmandu	0.39	0.35
2	Pokhara	0.29	0.30
3	Gorkha	0.26	0.30
4	Illam	0.42	0.40
5	Birgunj	0.31	0.30
6	Janakpur	0.29	0.30
7	Dhangadi	0.37	0.40
8	Darchula	0.30	0.35
9	Dadeldhura	0.36	0.35
10	Taplejung	0.25	0.30

4. Conclusions

PSHA of Nepal has been conducted using an earthquake catalogue of 123 years in the GEM OpenQuake engine. This involved creating a logical tree to minimize uncertainties in seismic sources and GMPEs. The analysis revealed that PGA values increase with longer return periods, reaching maximum levels in the far western and central regions due to their higher historical earthquake activity. ArcGIS was utilized to visualize earthquake hazard levels through colour ramping. The 475-year return period event, corresponding to a 10% probability of occurrence for 50 years, is widely used in most seismic building codes and designs and for seismic risk assessment.

The site-specific seismic hazard for KTP station was performed by considering three different source models i.e. areal source, linear source, and 3D source model for a 760-year return period. The results were then compared with the observed ground motion data pertaining to the Gorkha earthquake in 2015. A comprehensive study of all sources by comparison of PGA values at different probabilities of exceedance validates the Single Ramp Model of MHT for Nepal (3D source). In previous studies, the source models used to compute hazard do not consider the subduction source i.e. MHT and also the MHT has been modelled as one fault with no segmentation, so the measured PGA values are relatively higher. In this study, proper segmentation of subduction source, i.e. MHT as proposed by Elliott et al. (2016), is used.

PSHA, in this study, was performed considering the validated source model, i.e. Single Ramp Model, for MHT at the bedrock level. Future studies may consider incorporating data at ground level. In addition, analysis of the effect of combining the various source models can provide an enhanced perspective on the values of PGA and hazard maps that can be obtained.

Acknowledgements

The authors are thankful to the Department of Civil Engineering, IOE, Pashchimanchal Campus for providing a suitable platform to conduct this study.

Declaration of competing interests

The authors declare that they have no known competing financial interests or personal relationships that could have appeared to influence the work reported in this paper.

References

Algermissen, S.T., Perkins, D.M., Thenhaus, PC., Hanson, S.L. and Bender, B.L., (1982). Probabilistic estimates of maximum acceleration and velocity in rock in the contiguous United States. U.S. Geol. Surv., Open-File Rep., 82-1033, 99 pp.

Ambraseys, N. N., & Douglas, J. (2004). Magnitude calibration of north Indian earthquakes. Geophysical Journal International, 159(1), 165–206.

Baker, J., Bradley, B., & Stafford, P. (2021). *Seismic Hazard and Risk Analysis*. Cambridge: Cambridge University Press.

Bhusal, B., & Parajuli, H. (2020). Probabilistic Seismic Hazard Analysis for Nepal Using Areal and Longitudinal Faults Source. Journal of Nepal Geological Society, 61, 1-10.

Boncio, P., Lavecchia, G., & Pace, B. (2004). Defining a model of 3D seismogenic sources for Seismic Hazard Assessment applications: The case of central Apennines (Italy). Journal of Seismology, 8(3), 407–425.

Chamlagain, D., & Niroula, G. P. (2020a). Contribution of Fault Geometry on Probabilistic Seismic Hazard Assessment in Intermontane Basin: An example from Kathmandu Valley. Journal of Nepal Geological Society, 60, 21–36.

Chamlagain, D., Niroula, G., Maskey, P., Bista, M., Tamrakar, M., Gautam, B., Ojha, S., Dhakal, R., & Acharya, I. (2019). Probabilistic seismic hazard assessment of Nepal for revision of national building code (NBC)-105. Journal of Nepal Geological Society, 59, 1-14.

Chaulagain, H., Gautam, D., & Rodrigues, H. (2018). Revisiting Major Historical Earthquakes in Nepal. In Impacts and Insights of Gorkha Earthquake in Nepal (pp. 1–17). Elsevier.

Cornell, C. A. (1968). Engineering seismic risk analysis. Bulletin of the Seismological Society of America, 58(5), 1583-1606.

Dezes, P. (1999). Tectonic and metamorphic evolution of the central Himalayan domain in southeast Zanskar (Kashmir, India) (No. 32). Universite de Lausanne.

Elliott, J. R., Jolivet, R., Gonzalez, P. J., Avouac, J. P., Hollingsworth, J., Searle, M. P., & Stevens, V. L., (2016a). Himalayan megathrust geometry and relation to topography revealed by the Gorkha earthquake. Nature Geoscience, 9(2), 174–180. https://doi.org/10.1038/ngeo2623

Gansser, A. (1964). Geology of The Himalayas.

Gardner, J.K. and Knopoff, L., (1974). Is the sequence of earthquakes in Southern California, with aftershocks removed, Poissonian? Bulletin of the Seismological Society of America, v. 64(5), pp.1363-1367.

Ghimire, S. (2017). Probabilistic seismic hazard analysis of Nepal. Journal of Nepal Geological Society, 55, 29-38.

Ghimire, S. (2019). Probabilistic seismic hazard analysis of Nepal. Journal of Innovations in Engineering Education, 2(1), 199–206.

Ghimire, S., & Parajuli, H. R. (2016). Probabilistic Seismic Hazard Analysis of Nepal Considering Uniform Density Model.

Grünthal, G., and Wahlström, R. (2003). An MW based earthquake Catalogue for central, northern and northwestern Europe using a hierarchy of magnitude conversions. J. Seismol., 7(4), 507–531.

Hanks, T. C., & Kanamori, H. (1979). A moment magnitude scale. *Journal of Geophysical Research: Solid Earth*, *84*(B5), 2348-2350.

Hubbard, J., Almeida, R., Foster, A., Sapkota, S. N., Bürgi, P., & Tapponnier, P. (2016). Structural segmentation controlled the 2015 M_w 7.8 Gorkha earthquake rupture in Nepal. Geology, 44(8), 639–642.

Kaviris, G., Papadimitriou, P., Chamilothoris, L., and Makropoulos, K. (2008). Moment magnitudes for small and intermediate earthquakes. In Proceedings of the 31st General Assembly of the European Seismological Commission. ESC.

Khanal, R., Shrestha, R., Chhetri, P., & Pradhan, B. (2023). Seismicity parameters of Nepal by cumulative slope point change method. Journal of Engineering Issues and Solutions, 2(1), 138–149. https://doi.org/10.3126/joeis.v2i1.49450

Medina, F., Harmsen, S. C., & Barrientos, S. E. (2017). Probabilistic seismic hazard analysis for Chile. In 16th World Conf. on Earthquake Engineering.

Monsalve, G., Sheehan, A., Schulte-Pelkum, V., Rajaure, S., Pandey, M. R., & Wu, F. (2006). Seismicity and one-dimensional velocity structure of the Himalayan collision zone: Earthquakes in the crust and upper mantle. Journal of Geophysical Research, 111(B10). doi:10.1029/2005jb004062

Nath, S. K., Mandal, S., Das Adhikari, M., & Maiti, S. K. (2016). A unified earthquake catalogue for South Asia covering the period 1900–2014. Natural Hazards, 85(3), 1787–1810. doi:10.1007/s11069-016-2665-6

Niroula, G., & Chamlagain, D. (2021). Contribution of fault geometry to probabilistic seismic hazard in intermontane basin: An example from Kathmandu Valley. Journal of Asian Earth Sciences, 214, 104748.

Pandey, M. R., Tandukar, R. P., Avouac, J. P., Vergne, J., & Heritier, T. (1999). Seismotectonics of the Nepal Himalaya from a local seismic network. Journal of Asian Earth Sciences, 17(5-6), 703-712.

Parajuli, H. (2015). Seismic hazard estimate of Kathmandu. Unpublished Doctoral Dissertation, Kyoto University, Japan.

Poudyal, D., & Gupta, K. (2021). Detailed probabilistic seismic hazard analysis of Kathmandu Valley, Nepal. Journal of Earthquake Engineering, 1-22.

Upreti, B. N. (1999). An overview of the stratigraphy and tectonics of the Nepal Himalaya. Journal of Asian Earth Sciences, 17(5–6), 577–606.

Mcguire R.K. (2004). Seismic hazard and risk analysis. Earthquake Engineering Research Institute, MNO-10.

Rahman, M., & Bai, L. (2018). Probabilistic seismic hazard assessment of Nepal using multiple seismic source models. Journal of Earthquake Engineering, 22(1), 1-20.

Ram, T. D., & Wang, G. (2013). Probabilistic seismic hazard analysis in Nepal. Earthquake Engineering and Engineering Vibration, 12(4), 577–586.

Reasenberg P., (1985). Second-order moment of Central California seismicity, 1969–1982. J Geophys Res 90:5479–5495.

Reiter, L. (1990): Earthquake Hazard Analysis - Issues and Insights, 254 S. New York, (Columbia University Press).

Scordilis, E. M. (2006). Empirical global relations converting M_S and M_b to moment magnitude. J. Seismol., 10(2), 225–236

Searle, M. P., & Treloar, P. J. (2019). Introduction to Himalayan tectonics: a modern synthesis. Geological Society, London, Special Publications, 483(1), 1-17.

Shrestha, S. (2014). Probabilistic seismic hazard analysis of Kathmandu City, Nepal. International Journal of Engineering Research and General Science, 2 (1).

Stepp, J. (1992). Analysis of completeness of earthquake sample in Pudet sound area and its effect on statistical estimates of earthquake hazard. Proceedings of the first micro zonation conference (pp.897-910).

Stevens, V. L., Shrestha, S. N., & Maharjan, D. K. (2018). Probabilistic Seismic Hazard Assessment of Nepal. Bulletin of the Seismological Society of America, 108(6), 3488–3510.

Tinti, S., and Mulargia, F. (1985). An improved method for the analysis of the completeness of a seismic catalogue. Lett. Nuovo Cimento, 42(1), 21–2

Annex 1 Source characterization

These annexes show the spatial variation of different source models considered by different researchers while performing the PSHA of Nepal.

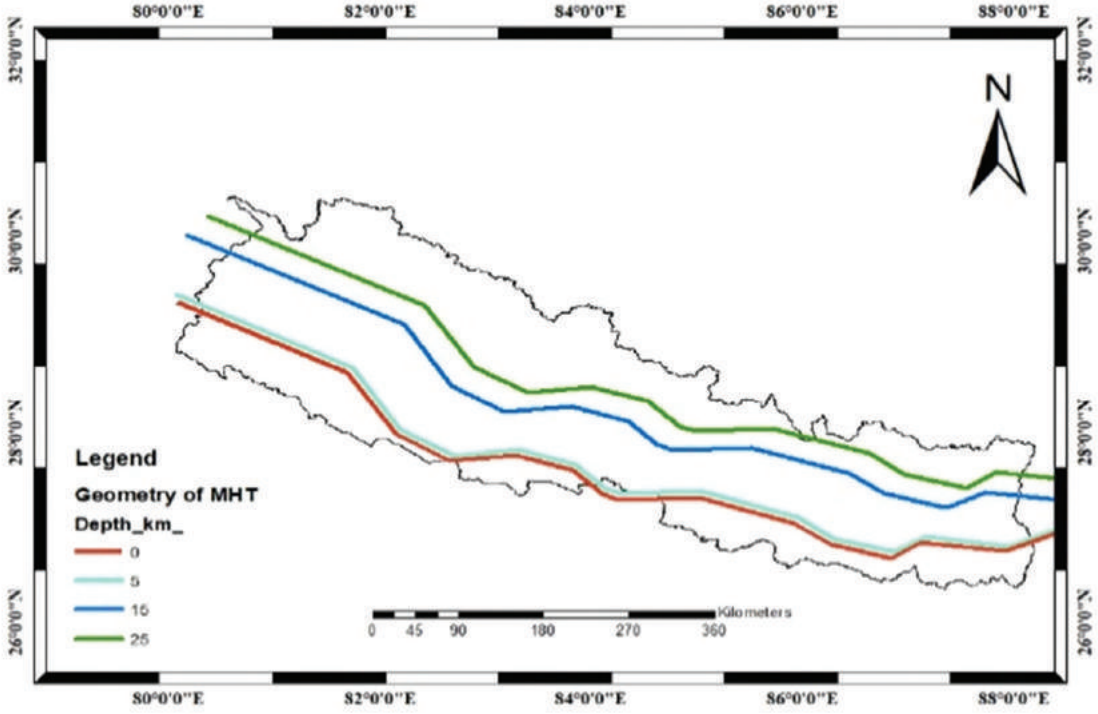

Figure A-1-1: Geometry of MHT (subduction interface) as per Niroula & Chamlagain (2020)

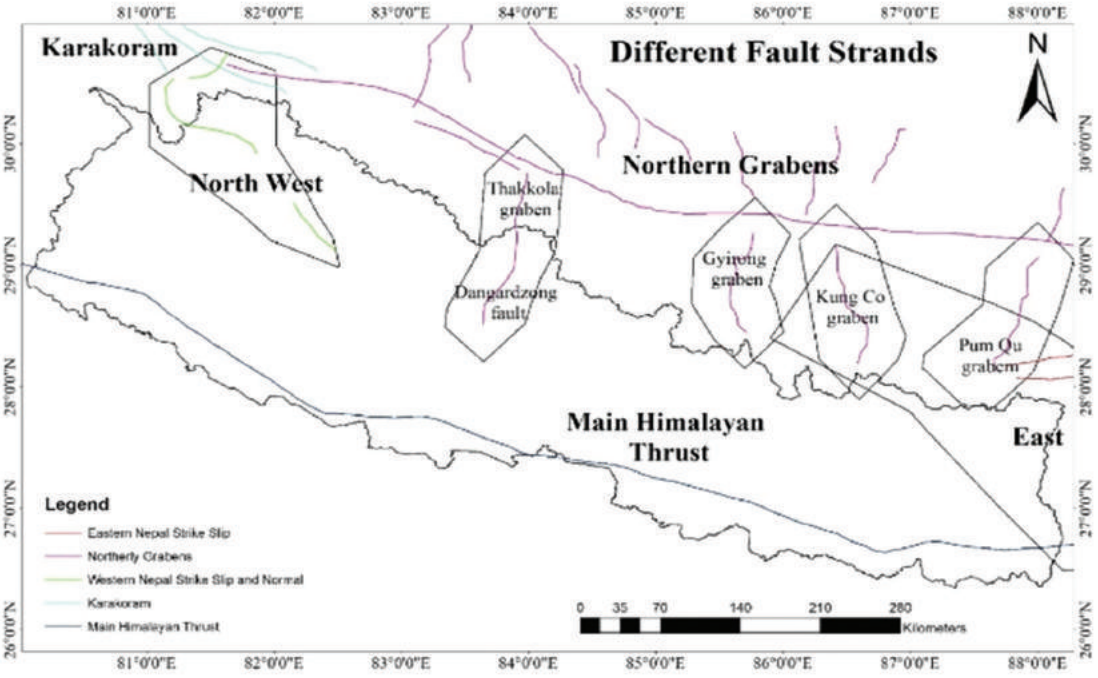

Figure A-1-2: Fault traces as per Stevens et al. (2018)

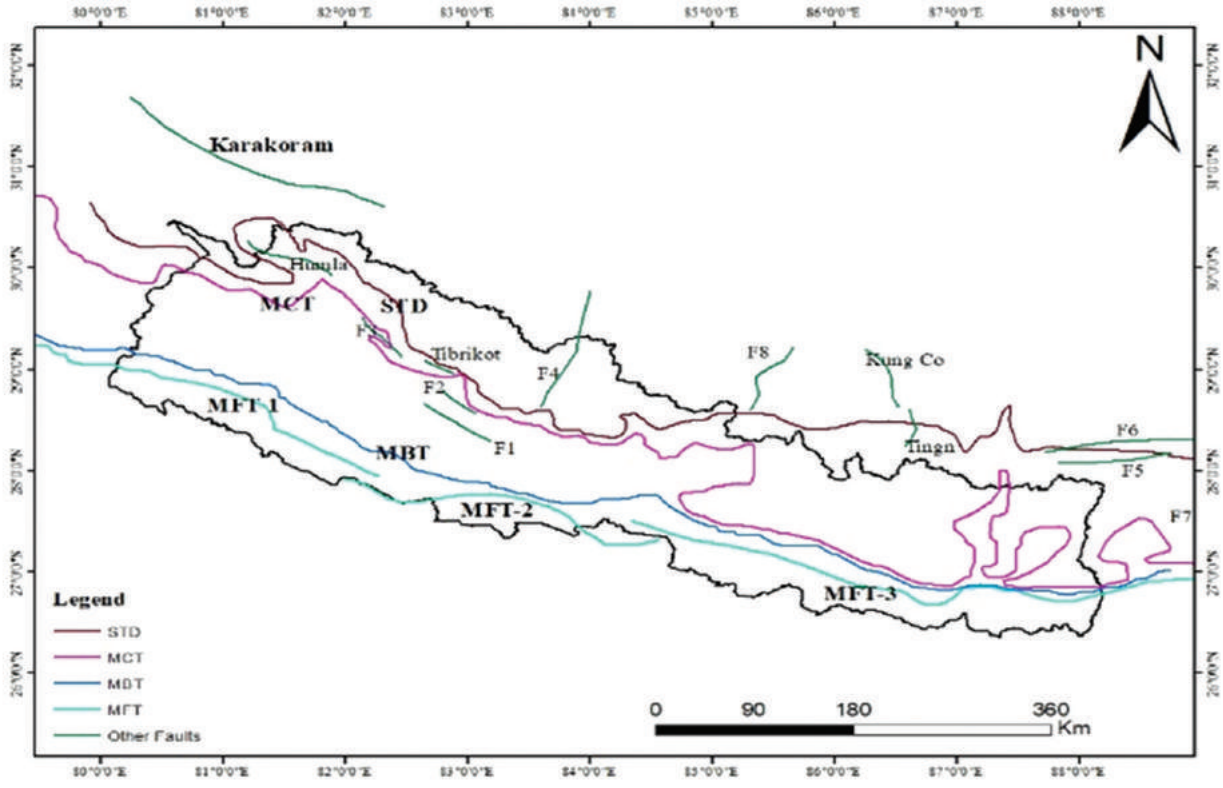

Figure A-1-3: Fault traces as per Rahman and Bai (2018).

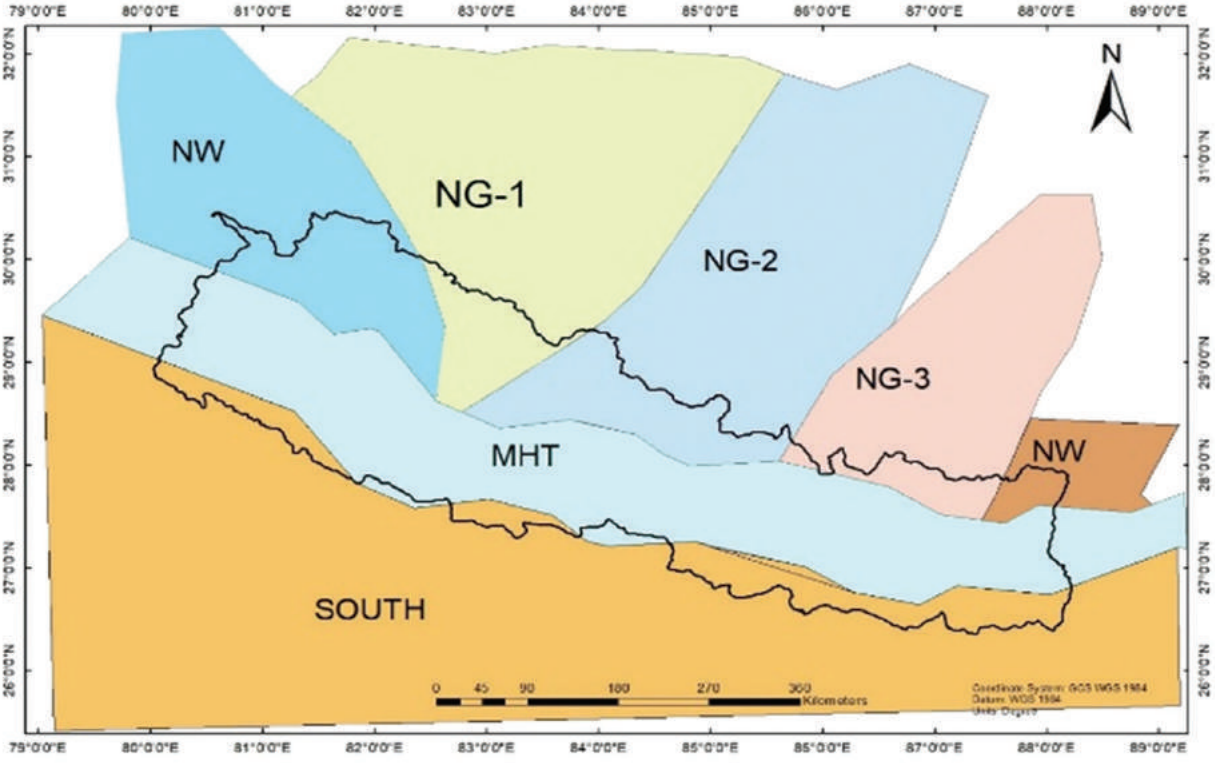

Figure A-1-4: Areal sources as per Niroula and Chamlagain (2020).

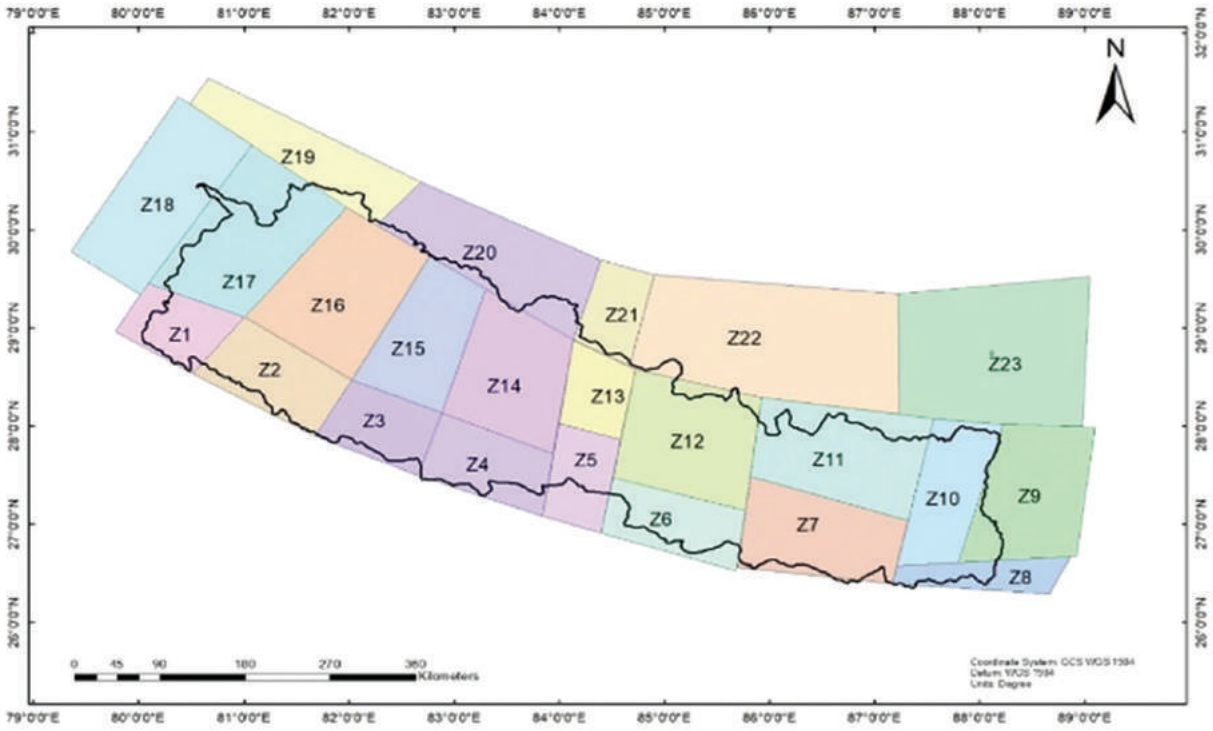

Figure A-1-5: Areal sources as per Ghimire and Parajuli (2016).

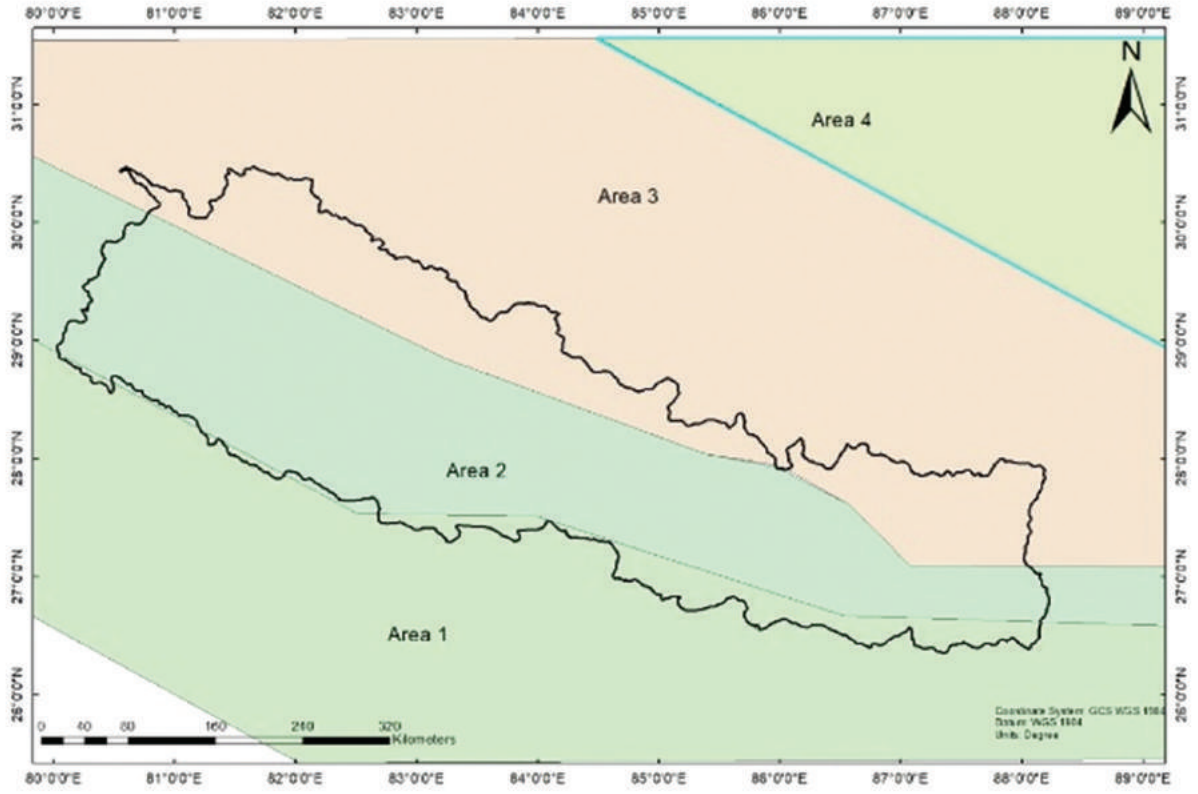

Figure A-1-6: Areal sources as per Chaulagain (2015)

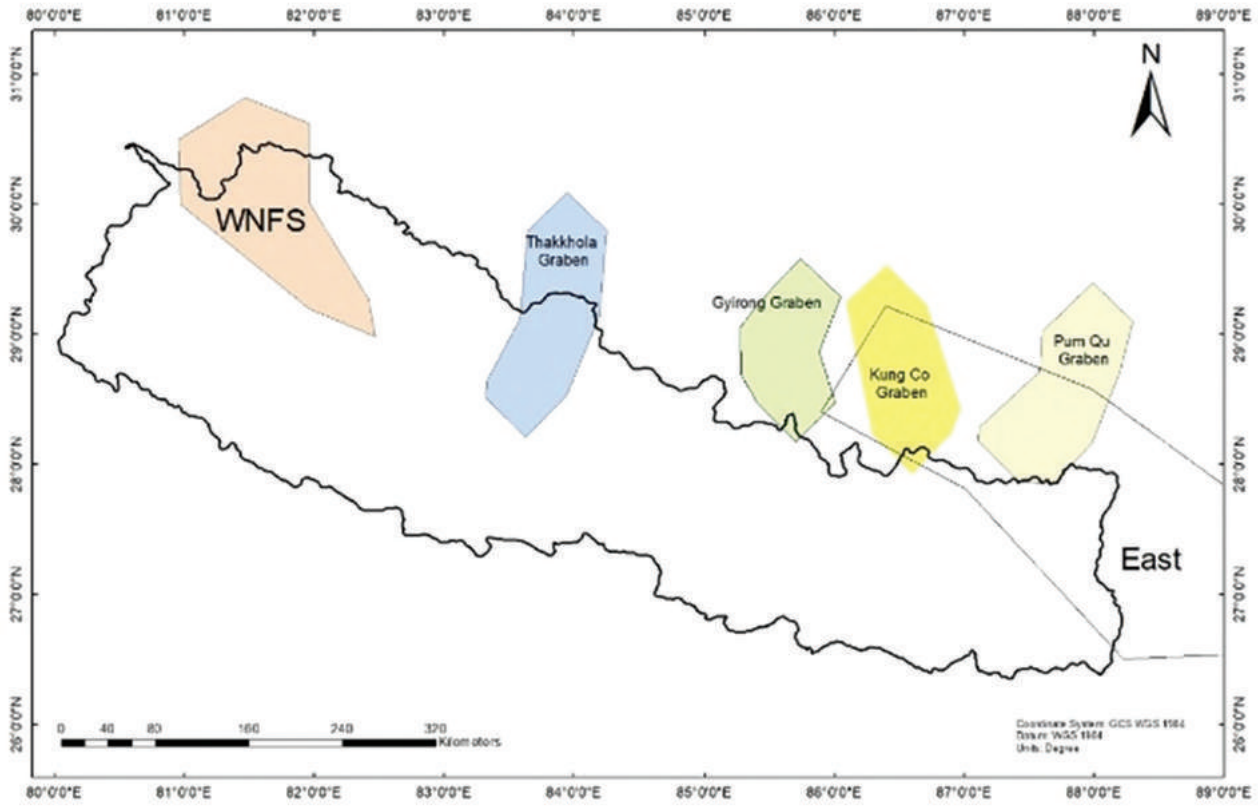

Figure A-1-7: Areal Sources as per Stevens et al. (2018)